Antennas for the Next Generation of Low-Frequency Radio Telescopes

Steven W. Ellingson, *Senior Member, IEEE*

***Abstract*—The next generation of large telescopes for radio astronomy at frequencies below 100 MHz will consist of tens of thousands of wide-band dipole-like antennas, each individually instrumented with a receiver and combined using digital signal processing. At these frequencies, the sensitivity of a telescope is limited by Galactic noise, with the result that even simple dipoles can deliver extraordinary useable bandwidth. In this paper the necessary characteristics for these antennas are explained, some bounds on performance are developed, and a few candidate designs are analyzed. It is shown that antenna systems consisting of simple wire dipoles, a 360 K active balun, and a long coaxial feedline can achieve Galactic noise-limited performance over large portions of the range 10–100 MHz. It is further shown that when these antennas are used as elements in a compact array, their Galactic noise-limited characteristics are not significantly affected.**

***Index Terms*—Antenna array, dipole, radio astronomy.**

I. Introduction

In radio astronomy, "low frequency" usually refers to the spectrum below $\sim$100 MHz. Historically, this band has received relatively little attention from astronomers. This is due largely to the complications imposed by the Earth's ionosphere, which becomes increasingly refractive and turbulent below 100 MHz, and becomes essentially opaque below 10 MHz. Also, "filled aperture" antennas (typically paraboloidal reflectors) which are commonly used as interferometer elements at higher frequencies become impractically large below 100 MHz; therefore beamforming arrays consisting of many low-gain elements must be used instead. Examples of such arrays include the 22-MHz narrowband dipole array at Penticton, British Columbia, active during the 1960s [1]; UTR-2, a 10–25 MHz array of "fat" dipole elements built in Ukraine during the 1970s [2]; and the Clark Lake Teepee-Tee (TPT), a 15–125 MHz array consisting of conical spiral antennas built in Southern California during the 1970s [3]. Interest in observations at these frequencies ebbed in the 1980s, mostly due to the superior imaging resolution then possible at higher frequencies.

Several factors have contributed to revived interest in low-frequency radio astronomy. In the early 1990s a technique was developed which dramatically improved astronomers ability to mitigate the effects of the ionosphere in aperture synthesis imaging, allowing resolution on the sub-arcminute scale for the first time [4]. Over the same time frame, cost and technology for receivers and digital signal processing suitable for large beamforming arrays improved dramatically, making it reasonable to consider building arrays much larger than previously attempted. In addition, an increasing number of questions in astrophysics and cosmology have emerged in which low-frequency radio astronomy may play an important or essential role [5].

At present, at least three new large telescope projects are underway: The Low Frequency Array (LOFAR), now in an advanced prototyping phase in the Netherlands [6]; the Long Wavelength Array (LWA), which is planned to be built in New Mexico and for which two prototype systems are now being designed [5], [7]; and the Mileura Wide-Field Array (MWA), planned to be built in Western Australia [8]. All of these instruments require tens of thousands of antenna elements, each having broad beamwidth and the largest possible bandwidth. Each element is to be individually received, digitized, and then combined by beamforming into groups of on the order of hundreds of elements, referred to as "stations." Each station is the functional equivalent of a large dish antenna in a traditional (higher frequency) aperture synthesis radio telescope, and at this level are combined to form images. The extraordinarily large number of antennas required makes it essential that each antenna has the lowest possible cost; is easy to manufacture and install; and is rugged, preferably requiring no maintenance.

To achieve large tuning range, previous telescopes such as UTR-2 and TPT used antennas which have inherently large bandwidth, in the sense that the terminal impedance is nearly constant over a large frequency range. Unfortunately, such antennas (including "fat" dipoles and conical spirals) are mechanically complex, making them expensive, difficult to construct, and prone to maintenance problems. This makes them unsuitable as elements in arrays on the scale of LOFAR, LWA, and MWA. In contrast, simple wire dipoles are mechanically very well suited for use in large low-frequency arrays, but have inherently narrow impedance bandwidth. However, this is not as strict a limitation at low frequencies as it is at higher frequencies: This is because natural Galactic noise can easily dominate over the self-noise of the electronics attached to the antenna. In this case, the antenna performance is unacceptable only if the impedance mismatch between the antenna terminals and the electronics becomes so great that the antenna system is no longer Galactic noise-limited. Once the antenna system is "minimally" Galactic noise-limited, further improvement in impedance match has little effect on the sensitivity of the instrument. Since Galactic noise is broadband and distributed over the entire sky, any further improvement in the sensitivity

Manuscript received December 17, 2004; revised February 26, 2005. This work was supported in part by the U.S. Naval Research Laboratory under Subcontract UT 05-049 with the Applied Research Laboratories of the University of Texas at Austin.

The author is with the Bradley Department of Electrical and Computer Engineering, Virginia Polytechnic Institute and State University, Blacksburg, VA 24061 USA (e-mail: ellingson@vt.edu).

Digital Object Identifier 10.1109/TAP.2005.852281

of the telescope can therefore be achieved only by adding additional antennas (increasing effective aperture). Thus, even badly-mismatched antennas—such as thin dipoles far from resonance—may in fact yield the best possible sensitivity.

This concept has been known for many years. It is the basic principle of operation for electrically-short "active antennas," which are commonly used in HF (3–30 MHz) communications [9], in which case man-made noise typically plays the same role as Galactic noise. In 2000, Tan and Rohner [10] showed that this approach was also applicable to low frequency radio astronomy. However, their study did not quantify the limits of this approach; for example, it was not clear to what extent the design of the antenna and associated electronics actually limits the degree to which the signal could be Galactic noise-limited, and over what range of frequencies. Recently, Stewart *et al.* [11] have reported achieving Galactic noise-limited performance in the range 10–50 MHz using a dipole-like antenna with a simple active balun. This confirms that the concept is valid, but design rules and performance bounds still do not exist.

This paper addresses these issues through a theoretical model, developed in Section II, in which the performance of the antenna as part of a radio telescope array is easily analyzed. This yields some simple design rules concerning the relationship between Galactic noise intensity, impedance mismatch, and the noise temperature of the electronics attached to the antenna, as shown in Section III. In Sections IV and V, a simple thin wire "inverted-V" dipole and a slightly more complex "fat" wire dipole are analyzed in the system context and are found to have effective bandwidths which cover large portions of the low frequency radio astronomy spectrum. In Section VI, the satisfactory performance of the fat wire dipole as an element in a compact array of like elements is confirmed. Findings are summarized in Section VII.

II. System Model

The signal path for a single antenna in a low-frequency radio telescope array can be generically modeled using just three components: 1) the antenna itself; 2) a preamplifier located near the antenna, which possibly also serves as a balun (sometimes referred to as an "active balun"); and 3) a long feedline connecting the preamplifier output to a central location. The feedline connects to a receiver, which converts the preamplifier output into a digital signal. Noise from the preamplifier and feedline must not overwhelm the Galactic noise captured by the antenna if the result is to be Galactic noise-limited. Because Galactic noise and the system components have frequency-dependent behaviors, it is useful to analyze the performance of the antenna in terms of the power spectral density of the various noise contributions, as seen by the receiver. This is determined for each component as follows.

A. The Antenna

The role of the antenna is to transfer incident power, including Galactic noise and emissions from astronomical sources of interest, to the antenna terminals. The Galactic noise power can be described in terms of the intensity I_ν, having units of W m^{-2} Hz^{-1} sr^{-1}, integrated over the antenna pattern. The resulting power spectral density at the terminals of an antenna is given by

$$S_a = \frac{1}{2}\int I_\nu A_e d\Omega \quad [\text{W Hz}^{-1}] \tag{1}$$

where A_e is the effective aperture,[1] the integration is over solid angle, and the factor of $(1/2)$ accounts for the fact that any single polarization captures about half of the available power since Galactic noise is unpolarized. As explained in Appendix I, the intensity of Galactic noise can be modeled as being spatially uniform and filling the beam of the antenna. A requirement for the antennas considered for this application is that they have very broad beamwidth, such that A_e is approximately constant over most of the sky. Assuming antenna gain is very small at and below the horizon (a very good assumption, and verified later in this paper), (1) simplifies to

$$S_a \sim \frac{1}{2} I_\nu A_e \Omega \tag{2}$$

where Ω is beam solid angle. Although this is only an approximation to (1), it is difficult to improve accuracy by using the original equation. This is because the small diurnal variation in I_ν due to the movement of different regions of the Galaxy across the sky yields about the same uncertainty as the approximation used to obtain (2).

Let $G = e_r D$ be the directivity of the antenna, where D is directivity and e_r is efficiency. In this analysis, mechanisms which make $e_r < 1$ include loss due to the finite conductivity of the materials used to make the antenna, and the imperfect (nonperfectly-conducting) ground. Since

$$A_e = \frac{\lambda^2}{4\pi} G \quad \text{and} \quad \Omega = \frac{4\pi}{D} \tag{3}$$

we have $A_e \Omega = e_r c^2/\nu^2$ where ν is frequency and c is the speed of light. Therefore

$$S_a \sim \frac{1}{2} e_r I_\nu \frac{c^2}{\nu^2}. \tag{4}$$

It will be useful to express this power density in terms of an equivalent temperature. This is possible through the Rayleigh–Jeans law

$$I_\nu = \frac{2\nu^2}{c^2} k T_{\text{sky}} \tag{5}$$

where k is Boltzmann's constant (1.38×10^{-23} J/K), and T_{sky} is defined to be the antenna equivalent temperature corresponding to Galactic noise. Thus, we have

$$S_a \sim e_r k T_{\text{sky}} \quad \text{where} \quad T_{\text{sky}} = \frac{1}{2k} I_\nu \frac{c^2}{\nu^2} \tag{6}$$

and I_ν is given in Appendix I. T_{sky} is plotted in Fig. 1; note that this value ranges from ~200 000 K at 10 MHz to ~800 K at 100 MHz.

[1]It is noted that A_e accounts for the tendency of the antenna to reflect a portion of the incident power back into the sky.

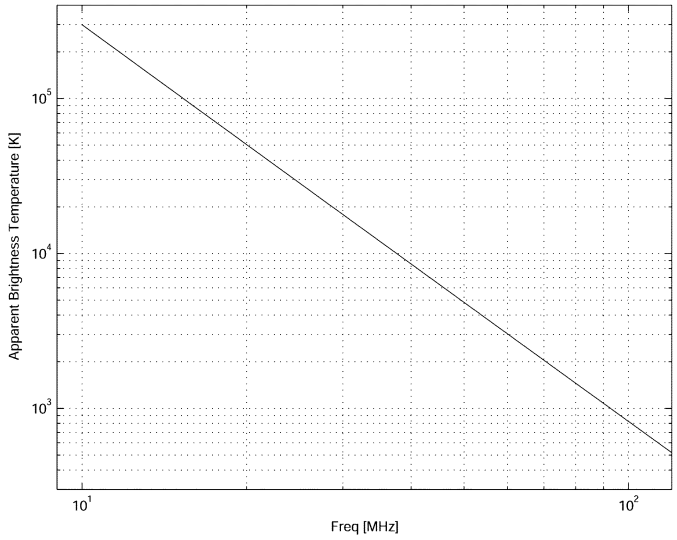

Fig. 1. Antenna temperture due to Galactic noise as received by a low-gain antenna.

B. The Preamplifier

The preamplifier is defined as the circuitry connected directly to the terminals of the antenna, whose purposes are typically to: 1) set the noise temperature of the system, and 2) buffer the impedance of the feedline from that of the antenna. Antennas for low-frequency radio astronomy (such as dipoles) will typically be balanced, whereas coaxial cable feedlines are unbalanced; thus, the preamplifier may also serve as a balun. In the analysis presented in the following sections, the preamplifier is described in terms of its input impedance $Z_{\rm pre}$, gain $G_{\rm pre}$, and noise temperature $T_{\rm pre}$. These parameters normally exhibit some frequency dependence, but the effect of this variation is typically insignificant compared to the effect due to the variation in the antenna impedance.

An issue which may deserve additional consideration is the dependence of $T_{\rm pre}$ on the impedance match at the preamplifier input. Since both the gain and noise characteristics of amplifiers are typically optimized for a specific input impedance, it is possible that a large mismatch may increase $T_{\rm pre}$ [12]. Physically, the situation is this: The noise power generated within the amplifier can be either: 1) transferred to the output, adding to $T_{\rm pre}$, or 2) it can be transferred to the input, corresponding to radiation from the antenna, which *reduces* $T_{\rm pre}$. Assume for the moment that the preamplifier is matched when the antenna is resonant. As frequency is decreased, eventually $|Z_a|$ is sufficiently large (capacitive) that the antenna is effectively an open circuit load to the preamplifier input, and therefore nearly all noise power is transferred to the output. Clearly this is the worst case scenario; on the other hand, any amplifier which achieves a useable noise temperature under this condition is assured to perform as well or better at higher frequencies.

Fortunately, this is known to be the case for at least two classes of amplifiers which are probably suitable for this application. Tan & Rohner [10] propose a "voltage sampling" approach which exploits the very large impedance at the gate input of a field effect transistor (FET). Amplifiers designed in this manner are known to be able to deliver noise temperatures below Galactic background levels in the 10–90 MHz range when used at the terminals of electrically-short antennas [9]. A second approach is to use commercial medium-power amplifiers designed for standard 50 Ω or 75 Ω input impedance. An example is the proof-of-concept demonstration reported by Stewart *et al.* [11], which employs an active balun constructed from two single-ended Motorola CA2830C amplifiers [13]. In independent testing, this inexpensive amplifier was verified to provide an noise temperature of 627 K independent of input impedance, even when open-circuited at the input [14].

To summarize, the dependence of $T_{\rm pre}$ on Z_a is technology-dependent and is difficult to model in a generic way. However, there exists at least two examples of amplifiers that produce noise which is sufficiently low over a large range of input impedance to be useful for low-frequency radio astronomy. In the event $T_{\rm pre}$ varies with Z_a, the analysis presented below provides conservative estimates of performance if $T_{\rm pre}$ is interpreted as an upper bound as opposed to an estimated value.

C. The Feedline

The feedline connects the preamplifier to the receiver, expected to be (but not necessarily) located tens or hundreds of meters away. The feedline is described in terms of G_f, which is the *gain* of the feedline such that G_f has a maximum of 1 (corresponding to a lossless line) and has a minimum value of zero. Feedline loss is frequency dependent, with loss increasing at higher frequencies.

III. Achieving Galactic Noise-Limited Operation

The primary requirement of the antenna-preamplifier-feedline system described above is that it delivers to the receiver a signal in which the dominant noise contribution is the unavoidable Galactic noise, i.e., is "Galactic noise-limited." As discussed in Section I, it is not necessarily desired to maximize power capture: Once the receiver input is Galactic noise-limited, further improvement in sensitivity can come only by increasing the total effective aperture of the station. This can be done by increasing the effective aperture of each antenna, or by increasing the number of antennas. Improvement in the effective aperture of each antenna can be achieved only by making the antenna more directional, which limits field-of-view and therefore is not desired. Thus, the only way to increase sensitivity is to use more antennas. For this reason, it is necessary only to achieve some threshold ratio of Galactic noise to self-generated noise at the output of each antenna-preamplifier-feedline assembly.

Determining the degree to which the receiver input is Galactic noise-limited requires knowledge of the other contributions to the system noise temperature. First, we consider the Galactic noise. Let S be the power spectral density due to $T_{\rm sky}$ at the output of the feedline. Given the above model for the system, one finds

$$S = e_r k T_{\rm sky}[1 - |\Gamma|^2] G_{\rm pre} G_f \tag{7}$$

where $1 - |\Gamma|^2$ is the fraction of power available at the antenna which is successfully transferred to the preamplifier. This fraction is nominally 1 but is often much less than 1 due to the impedance mismatch between antenna and amplifier. Γ is the

voltage reflection coefficient at the antenna terminals looking into the preamplifier and is given by

$$\Gamma = \frac{Z_{\rm pre} - Z_a}{Z_{\rm pre} + Z_a}. \tag{8}$$

Additional noise mechanisms include ground noise, which is the excess temperature due to that part of the antenna pattern which intercepts the surface of the Earth. A worst-case scenario is that of an isotropic antenna which intercepts a physical temperature of $\sim$290 K over the lower hemisphere of its pattern, adding $\sim$145 K to the antenna temperature. For this hypothetical antenna the antenna temperature due to Galactic noise is only $T_{\rm sky}/2$, which at 100 MHz is about three times greater than the ground noise contribution and increases dramatically with decreasing frequency. In practice, the ground tends to behave more like a reflector than as a blackbody (this is apparent in the patterns shown later in this paper), so the actual ratio is always much greater. Thus, it is reasonable to neglect the contribution of ground noise in this analysis.

Another noise mechanism to consider is the aggregate radio frequency din resulting from human activity, which is known to exhibit noise-like spectra. This noise is characterized in [15] in terms of four categories—"business," "residential," "rural," and "quiet rural." In each case, the associated noise power spectral density follows approximately the same power law as the Galactic noise, but with a different intercept point. The "quiet rural" scenario puts the associated temperature about a factor of about 5 below that of the Galactic noise, whereas the next quietest scenario, "rural," puts the temperature a factor of about 5 *above* the Galactic noise. The loudest scenario, "business," puts the temperature about a factor of about 30 above the Galactic noise. Although at first glance this might seem to be disastrous for low frequency radio astronomy, the effect in the worst case remains negligible because the man-made noise tends to be confined to within a few degrees of the horizon, and so will normally be completely outside a station beam which points toward the sky. The effect for individual receivers can be significant, however, as it is clear that man-made noise can potentially dominate over Galactic noise as seen by a single low-gain antenna. Because the effect is so highly variable and site-dependent, we shall simply note that an antenna system which is designed to be Galactic noise-limited may in fact actually be limited by man-made noise at some locations.

Undesirable noise is also generated by the preamplifier, which can be characterized in terms of the preamplifier's input-referenced noise temperature $T_{\rm pre}$. The resulting noise at the end of the feedline is

$$N_p = kT_{\rm pre}G_{\rm pre}G_f. \tag{9}$$

Finally, thermal noise arising from feedline loss may be significant. The noise delivered to the end of the feedline can be described in terms of the feedline's physical temperature $T_{\rm phys}$ as

$$N_f = kT_{\rm phys}[1 - G_f]. \tag{10}$$

The ratio γ of Galactic noise to undesirable noise measured at the end of the feedline is then

$$\gamma = \frac{S}{N_p + N_f}. \tag{11}$$

It will be demonstrated below that feedline noise can be made insignificant compared to preamplifier noise. In this case, we obtain

$$\gamma \approx e_r \frac{T_{\rm sky}}{T_{\rm pre}}[1 - |\Gamma|^2]. \tag{12}$$

The impedance match between antenna and preamplifier is often characterized in terms of the voltage standing wave ratio (VSWR), defined as

$$\rho = \frac{1 + |\Gamma|}{1 - |\Gamma|} \tag{13}$$

and therefore (12) can be written as

$$\gamma \approx e_r \frac{T_{\rm sky}}{T_{\rm pre}} \frac{4\rho}{(\rho+1)^2}. \tag{14}$$

This form is convenient because it reduces to a simpler expression for large VSWR, representing extremely badly matched antennas

$$\gamma \approx e_r \frac{T_{\rm sky}}{T_{\rm pre}} \frac{4}{\rho} \quad \rho \text{ large}. \tag{15}$$

These results place constraints on $T_{\rm pre}$ required for an antenna system to achieve a specified minimum γ, which we shall denote as $\gamma_{\rm min}$. These constraints are

$$T_{\rm pre} \leq e_r \frac{T_{\rm sky}(\nu_{\rm max})}{\gamma_{\rm min}} \quad \text{if} \quad \rho \sim 1 \tag{16}$$

and

$$T_{\rm pre} \leq e_r \frac{4T_{\rm sky}(\nu_{\rm max})}{\gamma_{\rm min}\rho} \quad \text{if} \quad \rho \gg 1 \tag{17}$$

where $\nu_{\rm max}$ is the highest frequency of operation. $\nu_{\rm max}$ is used because $T_{\rm sky}$ decreases with increasing ν. For a lossless ($e_r = 1$) antenna at $\nu_{\rm max} = 90$ MHz, $T_{\rm sky}(\nu_{\rm max}) \approx 1000$ K and $\gamma_{\rm min} = 4$ requires a preamplifier with $T_{\rm pre} \leq 250$ K if the antenna match is perfect, or $T_{\rm pre} \leq 100$ K for $\rho = 10$ (a badly matched but realistic antenna). Although $\gamma = 4$ is only just barely "Galactic noise-limited,"[2] note that γ increases rapidly with decreasing ν (due to the frequency dependence of $T_{\rm sky}$), so the mid-range γ will be very large.

Additional insight can be gained by considering the various contributions to the power spectral density at the feedline output separately, see Fig. 2. In this figure, S is shown for several fixed values of ρ; for example, the $\rho = 1$ curve corresponds to a hypothetical antenna that is perfectly matched at all frequencies. Although practical antennas do not have constant ρ over bandwidth, this plot is useful for understanding how good ρ

[2]In fact, specifications for LOFAR and LWA call for $\gamma \geq 10$ to ensure that required integration time is reduced to close to the minimum possible.

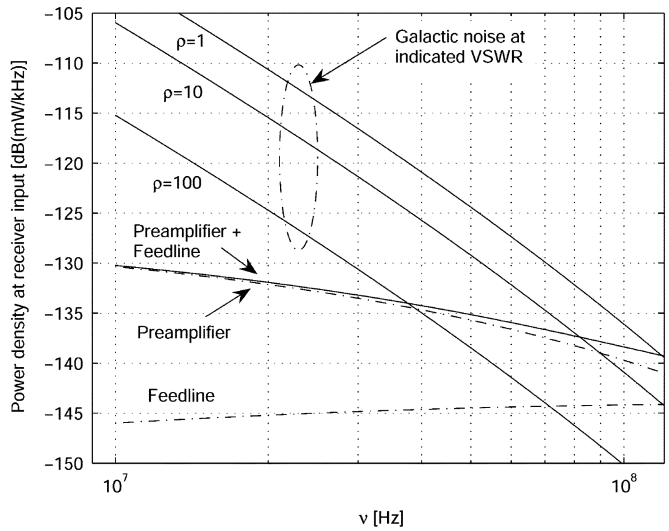

Fig. 2. Contributions to the power spectral density at the feedline output for a lossless antenna over a perfectly conducting ground plane ($e_r = 1$). In this plot, preamplifier gain and noise temperature are chosen to be $G_{\rm pre} = +17$ dB and $T_{\rm pre} = 360$ K, respectively. The "feedline" result assumes 152 m of RG-59 coaxial cable at $T_{\rm phys} = 290$ K, with associated G_f from -5 dB to -15.0 dB between 10 and 100 MHz, respectively.

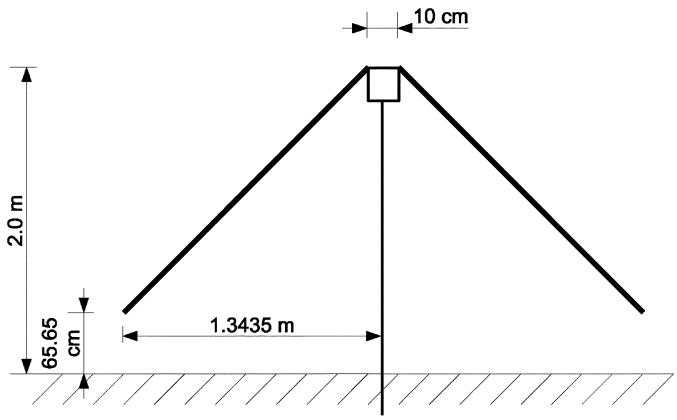

Fig. 3. Inverted-V dipole considered in Section IV.

must be at any given frequency to obtain Galactic noise-limited operation. We note that a very modest $T_{\rm pre}$—on the order of a few hundred degrees Kelvin—is sufficient to obtain very large γ even if the antenna is badly matched. This is due to the extreme brightness of the Galactic noise background. Another interesting observation is that for a given fixed ρ, the highest Galactic noise-limited frequency is determined by $T_{\rm pre}$. Finally, we note that the feedline noise contribution can be made negligibly small compared to the preamplifier noise, even for long sections of inexpensive coaxial cable.

IV. Example: A Thin Inverted-V Dipole

In this section, we consider a simple inverted V-shaped dipole shown in Fig. 3, which is an attractive candidate for large low-frequency radio telescope arrays due to its extreme simplicity and low cost. A family of similar designs is currently planned to cover the sub-100 MHz frequency range of LOFAR. The specific design considered here is constructed from inexpensive

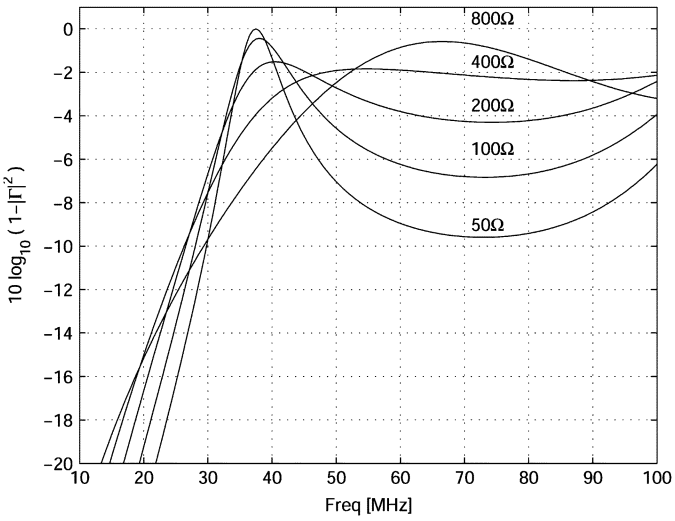

Fig. 4. Inverted-V dipole: Impedance mismatch efficiency for various values of $Z_{\rm pre}$, assuming lossy ground. The results for perfectly conducting ground are similar, with only a slight (≤ 0.5 dB) improvement above 50 MHz.

$1/2$-in copper pipe, which has an outside diameter of 15.85 mm. Each arm of the dipole is 1.9 m long, resulting in resonance at $\sim$38 MHz. Bending the arms downward at a 45° angle improves the pattern characteristics while lowering the terminal impedance to $\sim 50\ \Omega$ at resonance. Two such dipoles are placed at right angles with collocated feed points to obtain dual linear polarizations. This antenna was analyzed using NEC-2-based method-of-moments software. Two ground scenarios were considered: 1) realistic lossy ground having conductivity $\sigma = 5 \times 10^{-3}$ S/m and relative permittivity $\epsilon_r = 13$, and 2) perfectly-conducting ground, approximating the use of wire mesh (or similar treatment) in the ground under the antenna to mitigate ground loss.

Fig. 4 shows the "impedance mismatch efficiency" $1 - |\Gamma|^2$, which is the fraction of power captured by the antenna that is accepted by a preamplifier with various input impedances $Z_{\rm pre}$. Notable is the tradeoff between low $Z_{\rm pre}$, yielding good matching at resonance; and high $Z_{\rm pre}$, which provides improved power transfer above resonance. If a fixed frequency-invariant $Z_{\rm pre}$ is required, it appears a value in the range 200 Ω–800 Ω is best.

Fig. 5 shows that the patterns are quite reasonable over the range 26–53 MHz. It remains to show over what part of this range Galactic noise-limited operation is obtained.

For the remainder of this paper we shall assume a preamplifier with a modest $T_{\rm pre} = 360$ K and $G_{\rm pre} = +17$ dB. Regarding $Z_{\rm pre}$, we shall consider even-integer multiples of 50 Ω (i.e., 50, 100, 200 Ω, and so on). We will also continue to assume commonly-availably low-cost RG-59-type coaxial feedline 152-m long, such that G_f ranges from about -5 to about -15 dB over the frequency range of interest.

For this configuration, Fig. 6 shows the relative contributions of the Galactic background, preamplifier noise, and cable loss as seen at the input of a receiver at the far end of the feedline. Note that the design is Galactic noise-limited over a frequency span tens of MHz wide for any of the values of $Z_{\rm pre}$ shown. For $Z_{\rm pre} = 400\ \Omega$, this antenna system has $\gamma \geq 10$ from 33 to

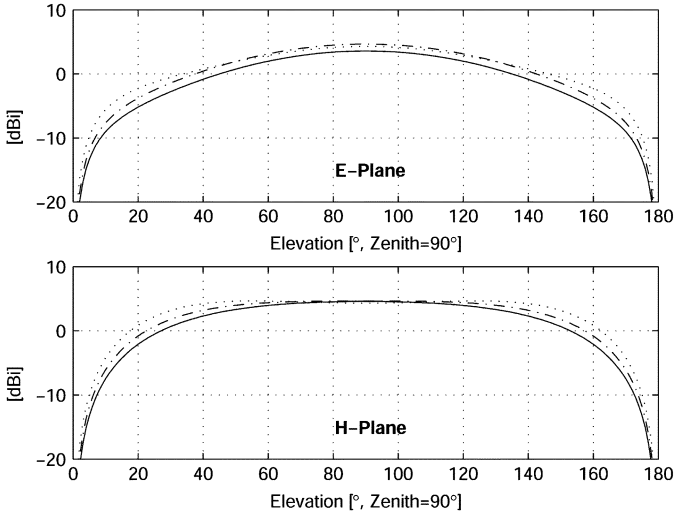

Fig. 5. Inverted-V Dipole: Copolarized patterns at 26 MHz (*Solid*), 38 MHz (*Dash-dot*), and 53 MHz (*Dot*). Assuming lossy ground conditions.

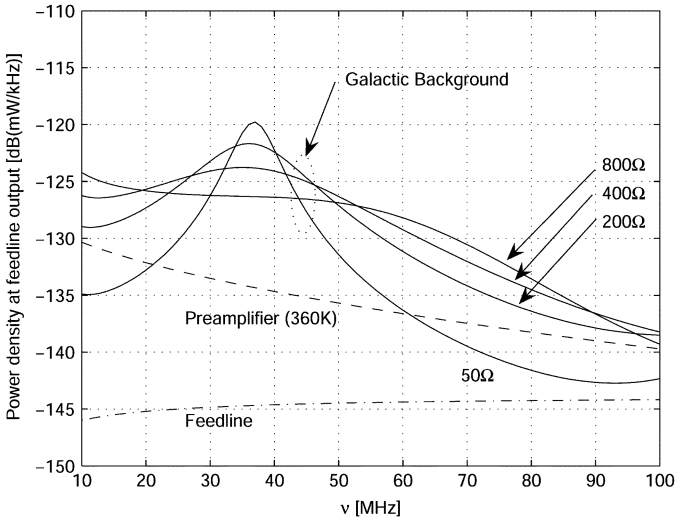

Fig. 6. Inverted-V dipole: Contributions to power spectral density at the feedline output, $e_r = 1$. Galactic background curves are for indicated values of $Z_{\rm pre}$.

46 MHz. If one is willing to accept $\gamma_{\rm min}$ to be reduced to $\sim$4, range of operation can be extended dramatically, from 19 to 66 MHz. These results confirm the perhaps counterintuitive result that the useful bandwidth of an antenna in this application may be much greater than is suggested by its very narrow impedance bandwidth when matched at resonance. Comparison to Fig. 2 further demonstrates that this high-impedance matching approach yields a result which is much closer to optimum than matching the antenna impedance at resonance, at high frequencies in particular.

The above result assumes no losses $(e_r = 1)$. In this study, the loss due to the finite conductivity of copper is negligable. Substituting a realistic ground, however, reduces e_r between 2.5 and 3.9 dB between 30 and 90 MHz. The result is nearly the same as shown in Fig. 6, except the Galactic Background curves are reduced by this much. This significantly reduces the useable bandwidth, and clearly demonstrates the value in the use

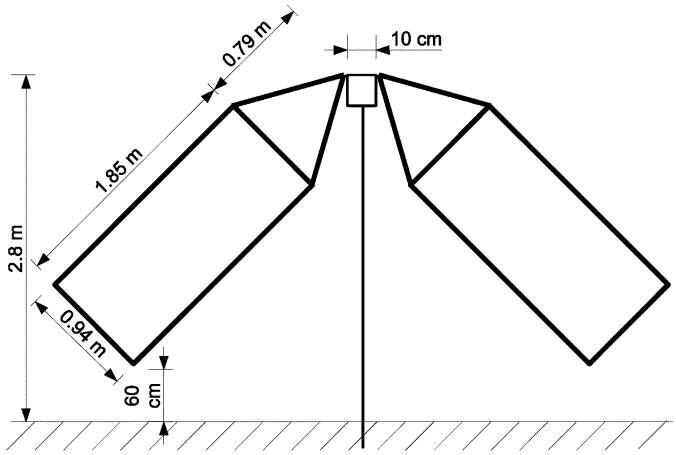

Fig. 7. NLTA dipole.

of treatments (such as installation of a wire mesh) to improve the effective conductivity of the ground beneath the antenna.

V. Example: The NLTA Dipole

Despite the surprisingly good performance of the thin inverted-V dipole, scientific motivation exists for achieving the largest possible tuning range. One possible strategy is to use multiple inverted-V dipoles of different sizes, with each covering part of the desired tuning range; this in fact is the strategy chosen for LOFAR. An alternative approach is to increase the useable bandwidth of a single antenna, which requires increasing the impedance bandwidth beyond that possible using a simple "thin" dipole. A well-known method for improving the bandwidth of dipoles is to make them "fat," that is, to increase the radiator thickness-to-length ratio [16]. It is also well-known that much of the benefit of thickness can be achieved by increasing the width only, resulting in a flat but wide radiator. Taken to an extreme, this structure can be approximated by a wire grid following the outline of a wide, flat radiator, resulting in a design which is easy to construct and has low wind loading.

Fig. 7 shows a candidate antenna of this type, currently in use at the U.S. Naval Research Laboratory's Low-frequency Test Array (NLTA), an eight-element prototype test facility located near Greenbelt, MD [11]. Like the inverted-V dipole, it is constructed from 15.85 mm copper pipe. The version considered here (unlike the actual NLTA elements) includes a second antenna at right angles to obtain dual linear polarization. The impedance mismatch efficiency for this antenna, using the same method of analysis and assumptions from Section IV, is shown in Fig. 8. In this case, it is noted that $Z_{\rm pre} = 200\ \Omega$ yields a good, approximately frequency-invariant match.

Fig. 9 is analogous to Fig. 6. Note that this antenna has dramatically better performance below 30 MHz, which is primarily due to its much larger size. This result is consistent with the findings of field tests of this design using a somewhat noisier (627 K) preamplifier [11].

Further extension of the useable bandwidth to higher frequencies would require that either $T_{\rm pre}$ be reduced or that the antenna size be reduced. Although appropriate preamplifiers

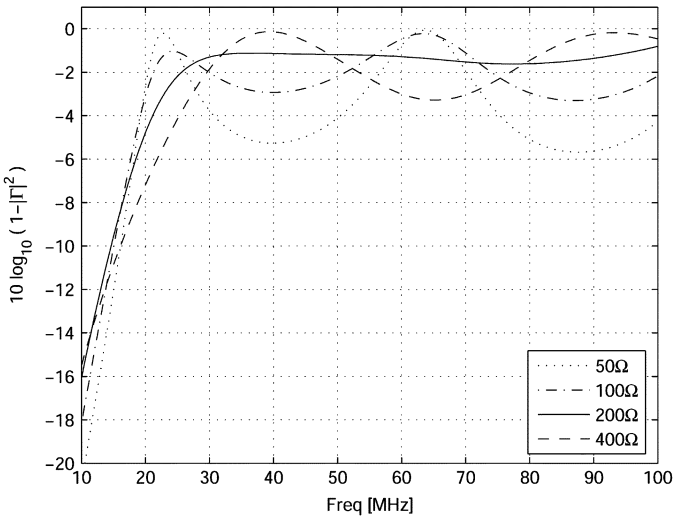

Fig. 8. NLTA dipole: Impedance mismatch efficiency for the indicated values of $Z_{\rm pre}$.

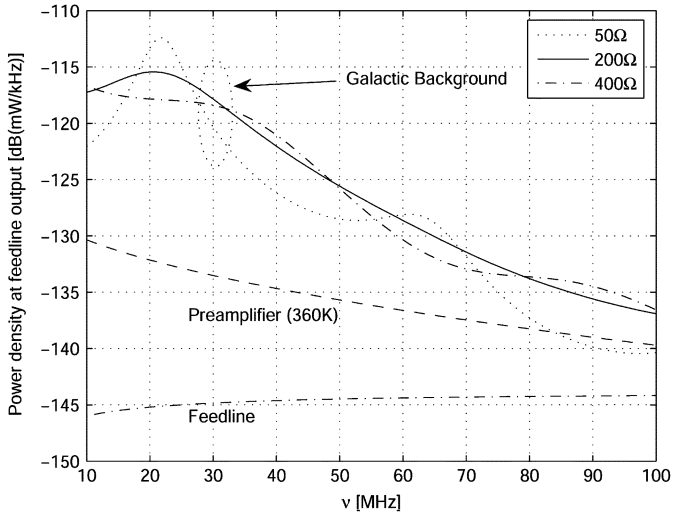

Fig. 9. NLTA dipole: Power spectral density at the feedline output, $e_r = 1$.

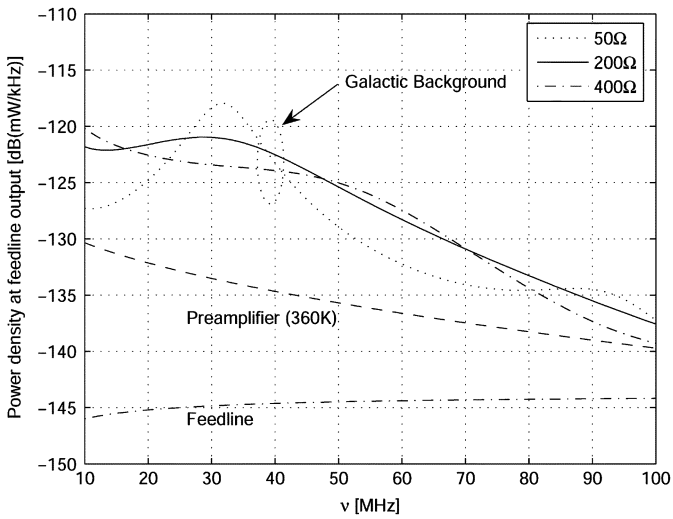

Fig. 10. NLTA dipole scaled by 0.68: Power spectral density at the feedline output $e_r = 1$.

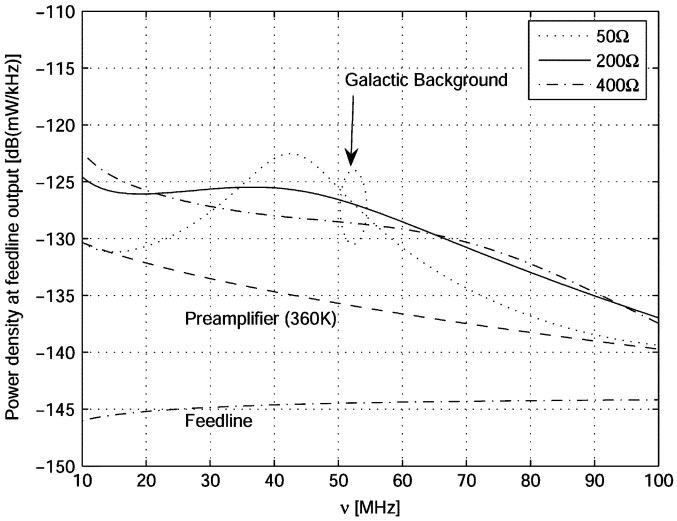

Fig. 11. NLTA dipole scaled by 0.5: Power spectral density at the feedline output $e_r = 1$.

with $T_{\rm pre}$ as low as 180 K have been demonstrated [17], this requires a somewhat more complex design and the benefit is reduced by feedline loss, which becomes increasingly important as $T_{\rm pre}$ is reduced. Thus, reducing antenna size is the more attractive strategy. Figs. 10 and 11 show the results when the antenna size (including height above ground) is scaled by factors of 0.68 and 0.5, respectively. It is noted that for $Z_{\rm pre} = 200\ \Omega$, the 0.68-scale version achieves the best overall performance: With respect to the smaller 0.5-scale antenna, it achieves approximately the same performance above 50 MHz (close to the theoretical bound established in Section III), but with better performance below 50 MHz. Its performance below 50 MHz is not as good as the 1.0-scale antenna, but is nevertheless sufficiently good to allow Galactic noise-limited performance, which is all that is required.

VI. Considerations for Array Elements

Although these antennas have applications in certain single-element or sparse array configurations, in a large radio telescope these antennas will be used as an elements in an compact array. To demonstrate that this reasonable, we now consider the 0.68-scale NLTA antenna as an element in a $5 \times 5 \times 2$-polarization uniform rectangular array in which the radiators for each polarization are arranged to be collinear. Let us assume that this array has spacing 3.24 m, which corresponds to 0.76 wavelengths at 74 MHz (the highest frequency band below 100 MHz allocated by federal regulation for radio astronomy), leaving 18 cm clearance between elements. $e_r = 1$ is assumed, implying some treatment (i.e., use of wire mesh) to improve the conductivity of the ground.

In this array, the mutual coupling resulting from close spacings leads to a small change in the antenna impedance which barely affects the mismatch efficiency. This is shown in Fig. 12. Thus, mutual coupling can effect performance only through changes in the antenna patterns. However, since antenna patterns do not significantly affect the reception of Galactic noise (see Section II-A), mutual coupling in this case has negligible

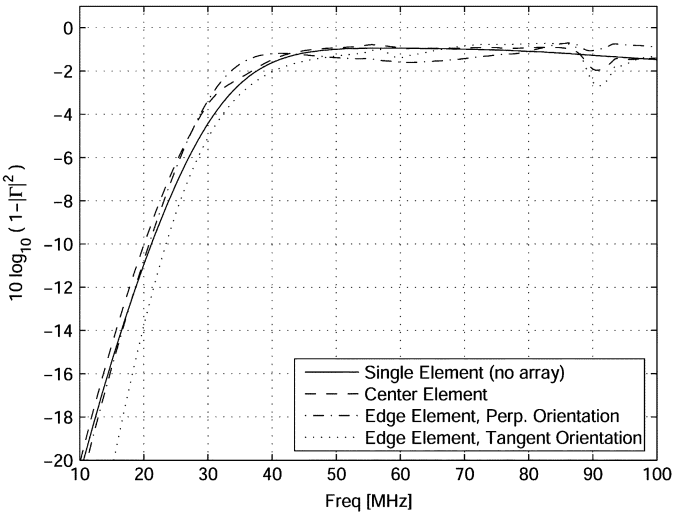

Fig. 12. Impedance mismatch efficiency of the 0.68-scale NLTA antenna as a standalone element, the center element of the array, and as an edge element of the array. $Z_{\rm pre} = 200\ \Omega$. "Perp." and "Tangent" refer to orientations in which the element is perpendicular and parallel, respectively, to the boundary of the array.

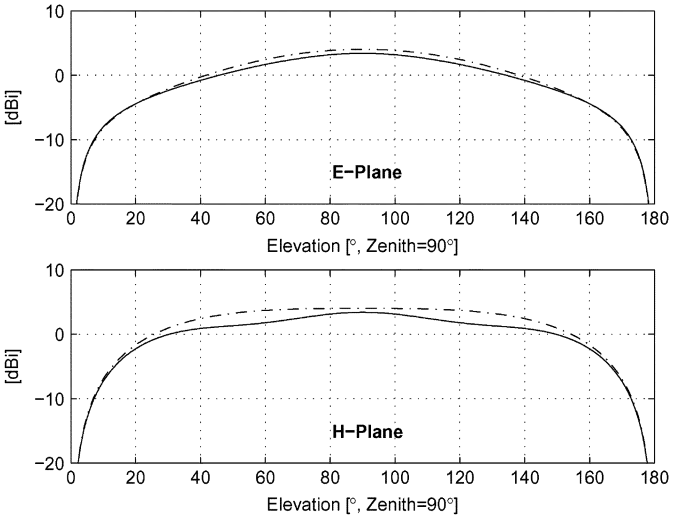

Fig. 13. Copolarized patterns at 38 MHz for the center element of the array (*Solid*) and an element alone (*Dash-Dot*).

effect on the degree to which individual elements are Galactic noise-limited.

However, the modification of element patterns due to mutual coupling is important for other reasons: First, recall that it is desired that the antenna have the broadest possible beamwidth. Second, it is important to know the effects so that they can be taken into account for beamforming. The patterns for a standalone element and the center element of the array at 38 and 74 MHz are shown in Figs. 13 and 14, respectively. The patterns for a standalone element and edge elements of the array at 38 and 74 MHz are shown in Figs. 15 and 16, respectively. As expected, it is found that mutual coupling can significantly alter the pattern: at 38 MHz, but the patterns remain broad and reasonably uniform, but significant degradation is evident in the 74 MHz patterns. This is a matter which should be addressed in future work.

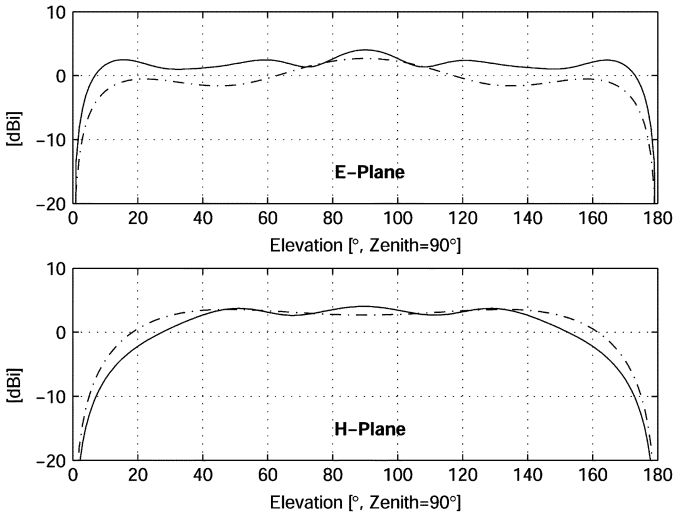

Fig. 14. Copolarized patterns at 74 MHz for the center element of the array (*Solid*) and an element alone (*Dash-Dot*).

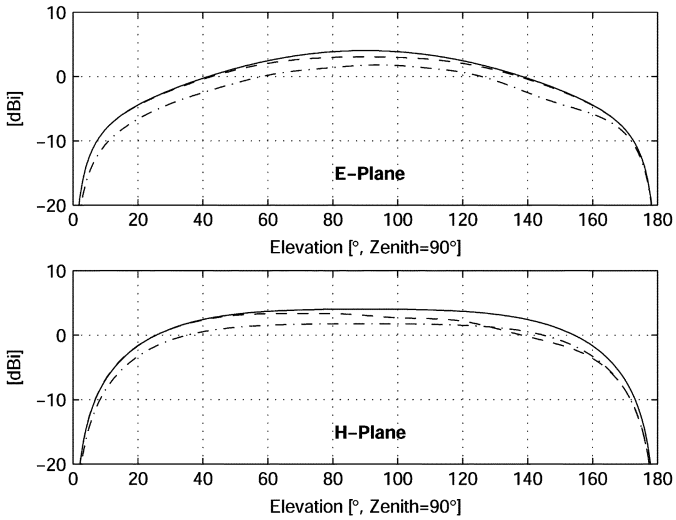

Fig. 15. Copolarized patterns at 38 MHz for a standalone element (*Solid*), edge element of the array in perpendicular orientation (*Dash-Dot*), and an edge element of the array in tangent orientation (*Dash*).

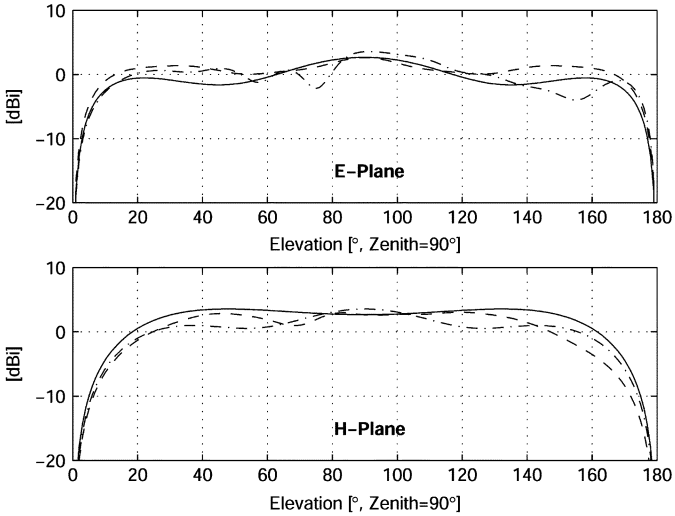

Fig. 16. Copolarized patterns at 74 MHz for a standalone element (*Solid*), edge element of the array in perpendicular orientation (*Dash-Dot*), and an edge element of the array in tangent orientation (*Dash*).

Antenna (scale)	Z_{pre} [Ω]	6 dB [MHz]	10 dB [MHz]	Width [m]
NLTA (1.00)	200	(< 10)–70	(< 10)–51	4.50
NLTA (0.68)	200	(< 10)–74	18–52	3.06
NLTA (0.50)	200	19–71	–	2.25
Inverted-V	400	19–66	33–46	2.69

Fig. 17. Summary of this study. Columns 3 and 4 show the frequency range over which the indicated antenna is Galactic noise-limited by the indicated factor (γ), assuming $e_r = 1$ and the indicated $Z_{\rm pre}$. "Width" refers to largest dimension in a direction parallel to the ground.

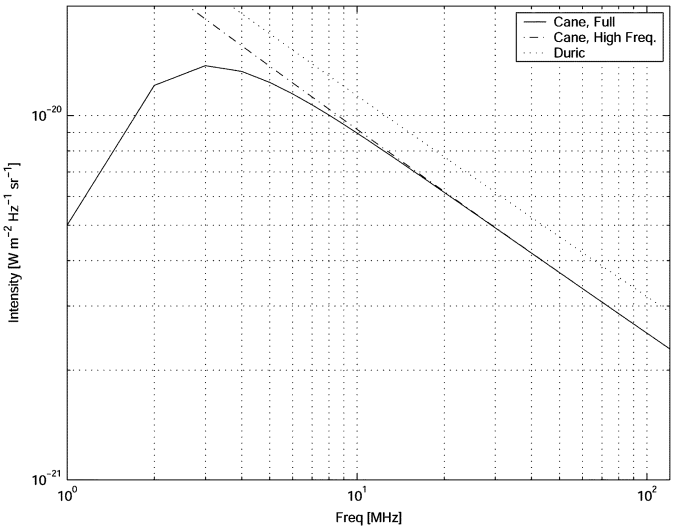

Fig. 18. Intensity of the Galactic radio background. *Solid*: Cane, *Dash-Dot*: High-frequency approximation to Cane (see text), *Dot*: Duric's modification to the high-frequency approximation.

VII. Conclusion

This paper has discussed some considerations in the design of antennas for modern low-frequency radio telescope arrays. These antennas are required to have the broadest possible beamwidth, Galactic noise-limited operation over the largest possible tuning range, and must be rugged, low cost, and mechanically simple. It is necessary to consider the impact of the preamplifier and feedline systems in the design and evaluation of these antennas; to this end some simple design criteria [(16) and (17)] were developed. Two candidate antennas were evaluated; a summary of findings is presented in Fig. 17. It is found that even the very simple antennas considered here are capable of achieving Galactic noise-limited operation over large portions of the 10–100 MHz range. It seems likely that some additional effort in optimization of the antenna design, matching circuits, and preamplifier noise temperature could result in further improvement of the performance without much increase in mechanical complexity.

Appendix I
Galactic Noise Spectrum

The spectrum of the Galactic noise background was quantified by Cane in 1979 [18], based on observations of the Galactic polar regions at four frequencies between 5.2 and 23.0 MHz. From these measurements, it was determined that the intensity is given in units of W m^{-2} Hz^{-1} sr^{-1} by

$$I_\nu = I_g \nu^{-0.52} \frac{1 - e^{-\tau(\nu)}}{\tau(\nu)} + I_{\rm eg} \nu^{-0.80} e^{-\tau(\nu)} \qquad (18)$$

where $I_g = 2.48 \times 10^{-20}, I_{\rm eg} = 1.06 \times 10^{-20}, \tau(\nu) = 5.0\nu^{-2.1}$, and ν in this case is frequency in MHz. In the above expression, the first term applies to the contribution from the Galaxy itself, whereas the second term accounts for extragalactic noise, which is assumed to be spatially uniform. This result is well-validated and in fact has been successfully employed to calibrate wide-field-of-view observations [19].

This result is plotted in Fig. 18. Note that the spectrum turns over at about 3 MHz and falls off in a log-linear fashion with increasing frequency above 10 MHz. Thus, a simpler expression for the spectrum above 10 MHz is simply

$$I_\nu \approx I_g \nu^{-0.52} + I_{eg} \nu^{-0.80} \qquad (19)$$

which is also plotted in Fig. 18.

This result applies to the Galactic poles. Since the noise intensity is correlated with the distribution of mass in the Galaxy, this result represents a broad minimum, whereas the noise in the direction of the Galactic plane is somewhat higher. However, because the Galactic plane remains spatially unresolved in low-gain antennas, the additional noise contribution is relatively small. A correction to the Cane high-frequency approximation proposed by Duric [20] based on the work of Tokarev [21] is simply to increase I_g to 3.2×10^{-20}, with the result shown in Fig. 18. Because the correction changes the result only slightly, and because the actual value is somewhat dependent on the beamwidth of the antenna and the location of the Galactic Center with respect to the antenna beam, the uncorrected Cane high-frequency approximation is used in this paper. As a result, the performance of antennas is probably slightly underestimated.

Additional information on the various contributions to the Galactic noise spectrum can be found in [21].

Acknowledgment

The author acknowledges very helpful discussions with W. C. Erickson (designer of the NLTA dipole) and J. R. Fisher, as well as the contributions of his students T. Kramer and D. Wilson on some of the topics discussed in this paper. Many of the ideas presented in this paper were initially considered by the Technical Advisory Committee of the international LOFAR project, which was chaired by the author between 2002 and 2003. Also, B. Hicks, N. Kassim, K. Stewart, and K. Weiler of the U.S. Naval Research Laboratory provided advice and prototype equipment which has been useful in confirming many of the ideas presented in this paper. Thanks also to T. Gaussiran of the University of Texas at Austin Applied Research Laboratories for that organization's support of this work.

References

[1] C. H. Costian, J. D. Lacey, and R. S. Roger, "Large 22-MHz array for radio astronomy," *IEEE Trans. Antennas Propag.*, vol. AP-17, no. 2, pp. 162–169, Mar. 1969.

[2] S. Ya. Braude *et al.*, "Decametric survey of discrete sources in the northern sky: I. The UTR-2 radio telescope. Experimental techniques and data processing," *Astrophys. Space Sci.*, vol. 54, pp. 3–36, 1978.
[3] W. C. Erickson, M. J. Mahoney, and K. Erb, "The Clark Lake Teepee-Tee telescope," *Astrophys. J. Supp. Ser.*, vol. 50, no. 403, pp. 403–420, Nov. 1982.
[4] N. E. Kassim, R. A. Perley, W. C. Erickson, and K. S. Dwarakanath, "Subarcminute resolution imaging of radio sources at 74 MHz with the very large array," *Astronomical J.*, vol. 106, pp. 2218–2228, 1993.
[5] N. E. Kassim and W. C. Erickson, "Meter- and decameter-wavelength array for astrophysics and solar radar," in *Proc. SPIE*, vol. 3357, July 1998, pp. 740–754.
[6] H. R. Butcher, "LOFAR: First of a new generation of radio telescopes," in *Proc. SPIE*, vol. 5489, Sep. 2004, pp. 537–44. See also web site http://www.lofar.org.
[7] [Online]. Available: http://lwa.nrl.navy.mil/
[8] [Online]. Available: http://web.haystack.mit.edu/MWA/
[9] U. L. Rhode and J. C. Whitaker, *Communications Receivers: DSP, Software Radios, and Design*, 3rd ed. New York: McGraw-Hill, 2001.
[10] G. H. Tan and C. Rohner, "Low-frequency array active-antenna system," in *Proc. SPIE*, vol. 4015, Jul. 2000, pp. 446–457.
[11] K. P. Stewart *et al.*, "LOFAR antenna development and initial observations of solar bursts," *Planetary & Space Sci.*, vol. 1352, no. 15, pp. 1351–55, Dec. 2004.
[12] G. Gonzalez, *Microwave Transistor Amplifiers: Analysis and Design*, 2nd ed. Englewood Cliffs, NJ: Prentice-Hall, 1997.
[13] *Wideband Linear Amplifiers: CA2830C*, 1997. Motorola Inc., (datasheet), CA2830C/D Rev. 1.
[14] W. C. Erickson, Univ. of Tasmania, Personal Communication, Feb. 2005.
[15] *Radio Noise*, 2003. International Telecommunications Union, ITU-R Rec. P.372-8.
[16] W. L. Stutzman and G. A. Thiele, *Antenna Theory and Design*, 2nd ed. New York: Wiley, 1998.
[17] R. Bradley, National Radio Astronomy Observatory, Personal Communication, Oct. 2003.
[18] H. V. Cane, "Spectra of the nonthermal radio radiation from the galactic polar regions," *Monthly Notice Royal Astronomical Society*, vol. 189, p. 465, 1979.
[19] G. A. Dulk *et al.*, "Calibration of low-frequency radio telescopes using the galactic background radiation," *Astron. & Astrophys.*, vol. 365, p. 294, 2001.
[20] N. Duric *et al.*. (2003) RFI Report for the U.S. South-West. [Online]. Available: http://web.haystack.mit.edu/lofar/rfi_download.html
[21] Y. Tokarev. Cosmic background with model of cloudy interstellar medium. presented at the VIII Russian-Finnish Symp. on Radioastronomy. [Online]. Available: http://www.gao.spb.ru/english/publ-s/viii-rfs/

Steven W. Ellingson (S'87–M'90–SM'03) received the B.S. degree in electrical and computer engineering from Clarkson University, Potsdam, NY, in 1987, and the M.S. and Ph.D. degrees in electrical engineering from the Ohio State University, Columbus, in 1989 and 2000, respectively.

From 1989 to 1993, he served on active duty with the U.S. Army, attaining the rank of Captain. From 1993 to 1995, he was a Senior Consultant with Booz-Allen and Hamilton, McLean, VA. From 1995 to 1997, he was a Senior Systems Engineer with Raytheon E-Systems, Falls Church, VA. From 1997 to 2003, he was a Research Scientist with the Ohio State University ElectroScience Laboratory. Since 2003, he has been an Assistant Professor in the Bradley Department of Electrical and Computer Engineering at Virginia Polytechnic Institute and State University, Blacksburg. His research interests include antennas and propagation, applied signal processing, and instrumentation.